World Academy of Science, Engineering and Technology
International Journal of Physical and Mathematical Sciences
Vol:3, No:10, 2009

Characterization of Responsivity, Sensitivity and Spectral Response in Thin Film SOI photo-BJMOS -FET Compatible with CMOS Technology

Hai-Qing Xie, Yun Zeng*, Yong-Hong Yan, Jian-Ping Zeng, Tai-Hong Wang

***Abstract*—**Photo-BJMOSFET (Bipolar Junction Metal-Oxide-Semiconductor Field Effect Transistor) fabricated on SOI film was proposed. ITO film is adopted in the device as gate electrode to reduce light absorption. Depletion region but not inversion region is formed in film by applying gate voltage (but low reverse voltage) to achieve high photo-to-dark-current ratio. Comparisons of photoelectric-characteristics executed among V_{GK}=0V, 0.3V, 0.6V, 0.9V and 1.0V (reverse voltage V_{AK} is equal to 1.0V for total area of $10\times10\mu m^2$). The results indicate that the greatest improvement in photo-to-dark-current ratio is achieved up to 2.38 at V_{GK}=0.6V. In addition, photo-BJMOSFET is compatible with CMOS integration due to big input resistance.

***Keywords*—**Photo-BJMOSFET, Responsivity, Sensitivity, Spectral response.

I. INTRODUCTION

NOWADAYS, short distance optical communications and emerging optical storage(OS) systems such as DVD applications require fast (gigahertz to tens of gigahertz bandwidth) and responsive photodetectors with high photo-to-dark-current ratio increasingly[1]-[5]. Bulk silicon detectors, however, hardly cope with these specifications, mainly in regards to bandwidth, and nonintegrated detectors are usually used due to high dark currents of photodiode and low sensitivity of MOS structure(due to only one kind of carrier and light-absorption of gate) in CMOS process under 0.25μm[6]-[9]. This limits the ultimate performances of optical receivers circuits because of high bonding capacitor, cost, and area, which is a limitation for the deployment of local-area networks, interchip/intrachip interconnects, and for the first mile ethernet[10].

Thanks to the particular silicon-on-insulator (SOI) structure, as will shown and can be expected. Thin-film SOI integrated detectors are excellent candidates to cope with speed and low dark current specifications [11],[12]. SOI technology has made large progress after the first SOI photodiode with a dark current of 0.1pA/1μm junction length was fabricated in laser-recrystallized SOI technique. A fast SOI photodiode with an area of $75\times75\mu m^2$ and a dark current of 10pA under a reverse bias of 5V was presented in a bonded and etched back (BESOI) technique [13].Lateral PIN photodiodes fabricated on SOI have been proposed recently. These diodes achieve a high responsivity and then combine all the advantages of high speed, low dark current, low capacitance (100times lower than bulk fingers photodiodes of the same area which are the photodiodes presently used in Blue DVD),and high sensitivity. Therefore, SOI thin-film lateral photodiodes are candidates of high interest for short distance optical communication [14]-[16]. However, device parameters of actual SOI CMOS processes, the intrinsic region, corresponding in fact to a P-doping of about $10^{15}cm^{-3}$. Thus, high reverse voltage must to be applied to achieve low dark current, high photocurrent and responsivity. Consequently, it is unable to cope with low-voltage operation. Furthermore, it isn't propitious to integration for the small input resistance. No results for photosensitive devices based MOS structure, however, have been reported so far.

In order to achieve low dark current and high photo-current under low reverse voltage, photo-BJMOSFET (Bipolar Junction Metal-Oxide- Semiconductor Field Effect Transistor) based on SOI film compatible with CMOS process is proposed presently. The structure of photo-BJMOSFET is very similar to traditional MOS structure, but only ITO is applied as gate to reduce light absorption. Recombination is reduced due to thin film is in depletion but not inversion region under gate voltage (but not high reverse voltage) to obtain low dark current and high photo-current. Consequently, it can get high sensitivity and responsivity. Furthermore, it is propitious to integration for big input resistance. These performances are sufficient to enlarge the applications of photosensitive device.

II. PRINCIPLE STRUCTURE ANALYSIS

Thin film SOI photo-BJMOSFET realized in 0.18μm SOI CMOS technology with the parameters depicted in Fig.1. It is shown that the structure is very similar to that of traditional NMOS except a P^+N injection junction is formed by using P^+ region instead of N^+ region as drain. In addition, ITO is adopted

Hai-Qing Xie is with the School of Physics and Microelectronics Science, Hunan University, Changsha 410082, P.R.China (e-mail: xiehaiqing@gmail.com).

Yun Zeng is with the School of Physics and Microelectronics Science, Hunan University, Changsha 410082, P.R.China (Tel.: +86 731 8822332; fax: +86 731 8822332 e-mail: zengyun@hnu.cn)

Yong-Hong Yan is with the School of Physics and Microelectronics Science, Hunan University, Changsha 410082, P.R.China (e-mail: yyh@hnu.cn).

as gate electrode to reduce the absorption loss of traditional gate. The thin Si film thickness, d_{si}, is equal to 200nm, the front oxide thickness, d_{FOX}, is equal to 100nm, the buried oxide (BOX) thickness, d_{BOX}, is equal to 380μm and the thickness of substrate, d_{sub}, is equal to 1μm. The length of the N^+ and P^+ zones, L_{PN}, is equal to 1μm and L, the length of the channel which typically corresponds to a P^--doping of $10^{15}cm^{-3}$, is equal to 8μm. In order to analyze the photoelectric characteristics, classical loss mechanisms and gate voltage influence must be taken into account and applied to our photo-BJMOSFET.

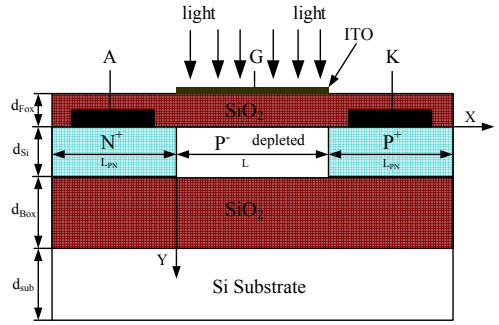

Fig. 1. Schematic cross-section of thin film SOI photo-BJMOSFET

2.1 Beam incident losses

Noting that P_{in} is the optical power density (by unit of area) incident to the photo-BJMOSFET, while P_{abs} is the part that is absorbed by the device along the thickness (d_{si}) of the collection area in the thin SOI film, the $\eta = \frac{P_{abc}}{P_{in}}$ ratio strongly depends on d_{si} , the wavelength of the incident light and the integrated loss due to absorption and reflection over the ray path and is a constant to L. Therefore, Generation Rate Formula is given by equation [17].

$$G = K\eta \frac{P_{in}\lambda}{hc}\alpha e^{-\alpha y} \tag{1}$$

where P_{in} is the optical power density (by unit of area), η is efficiency ratio, K is the internal quantum efficiency, which represents the number of carrier pairs generated per photon observed, y is a relative distance for the ray in question, h is Planck's constant, λ is the wavelength, c is the speed of light, α is the absorption coefficient in Silicon and is wavelength dependent.

The absorption in ITO electrode is the main loss of incident light. The deposition of ITO was performed in a vacuum chamber, where the preliminary pressure was 1×10^{-3}Pa. Sputtering was done at a pressure of 0.5Pa, at a constant power of 100W. During the sputtering process, the temperature of the substrates always was kept at 150 for 1.5 hours. Measurements of transmittancea to the wavelength of ITO film are presented in Fig.2. It can be seen that the transmittancea of ITO film is higher than 80% for λ from 500nm to 700nm, and can be adopted as gate electrode to reduce light absorption.

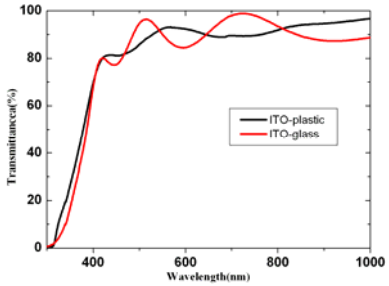

Fig. 2 Transmittancea to wavelength of ITO film which was deposited on glass and plastic, respectively, with thickness of 100nm.

2.2 Gate voltage analysis

In photo-BJMOSFET, the depletion but not inversion region is formed by V_{GK} under lower V_{AK} , the voltage between electrode A and electrode K, in channel to decrease dark current and increase internal quantum efficiency.

When no bias is applied ($V_{AK} = 0$), the charge per unit area in the semiconductor under oxide Q_C can be calculated using Gauss's law

$$Q_C = -\sqrt{2q\varepsilon_s N_A} \times \sqrt{V_t e^{-\psi_S/\phi_T} + \psi_S - \phi_T + e^{-2\phi_f/\phi_T}(\phi_T e^{\psi_S/\phi_T} - \psi_S - \phi_T)} \tag{2}$$

where q , ε_s , N_A , ψ_S , and ϕ_f are the magnitude of the electron charge, permittivity of the material, doping concentration, surface potential, and Fermi potential of the material, respectively. ϕ_T is thermal voltage and given by

$$\phi_T = \frac{kT}{q} \tag{3}$$

where k is the Boltzmann constant, T is the absolute temperature.

Expression for V_{GK} can be obtained using Kirchhoff's voltage law

$$V_{GK} = V_{FB} + \psi_S + \gamma\sqrt{\phi_T e^{-\psi_S/\phi_T} + \psi_S - \phi_T + e^{-2\phi_f/\phi_T}(\phi_T e^{\psi_S/\phi_T} - \psi_S - \phi_T)} \tag{4}$$

where V_{FB} is the flat-band voltage, the expressions for γ is as follows:

$$\gamma = \frac{\sqrt{2q\varepsilon_s N_A}}{C_{OX}} \tag{5}$$

with the oxide capacitance per unit area C_{OX} is given by

$$C_{OX} = \frac{\varepsilon_{OX}}{D_{OX}} \tag{6}$$

where D_{OX} is the thickness of the oxide and ε_{OX} is its permittivity.

When $V_{AK} > 0$, the surface potential at x position, $\psi_s(x)$, varies throughout the channel. In this condition, the charge per

unit area $Q_C^{'}$ in the semiconductor under oxide can be expressed

$$Q_C^{'} = -\sqrt{2q\varepsilon_s N_A} \times \sqrt{\phi_T e^{-\psi_S(x)/\phi_T} + \psi_S(x) - \phi_T + e^{-2\phi_f/\phi_T} \times (\phi_T e^{[\psi_S(x)-V(x)]/\phi_T} - \psi_S(x) - \phi_T e^{-V(x)/\phi_T})} \quad (7)$$

For the same reason, $V_{GK}^{'}$ can be written

$$V_{GK}^{'} = V_{FB} + \psi_S(x) + \gamma\sqrt{\phi_T e^{-\psi_S(x)/\phi_T} + \psi_S(x) - \phi_T + e^{-2\phi_f/\phi_T} \times (V_t e^{[\psi_S(x)-V(x)]/\phi_T} - \psi_S(x) - \phi_T e^{-V(x)/\phi_T})} \quad (8)$$

From (4) and (8), the ψ_S (or $\psi_s(x)$) can be obtained numerically for given V_{GK} and V_{AK} . Then, the width of depletion d_B ($V_{AK} = 0$) can be expressed

$$d_B = \sqrt{\frac{2\varepsilon_s}{qN_A}}\sqrt{\psi_s} \quad (9)$$

It is necessary to point out that the expression of $d_B(x)$ ($V_{AK} > 0$) is analogous to (9), but only the ψ_S is replaced by $\psi_S(x)$.

Additionally, it is worthwhile to note that the charge per unit area in the semiconductor under oxide Q_C is the sum of the charge due to the electrons in the inversion layer Q_L and the charge due to the ionized acceptor atoms in the depletion region Q_B :

$$Q_C = Q_L + Q_B \quad (10)$$

with

$$Q_B = qN_A d_B \quad (11)$$

Equation (12) is Boltzmann distribution

$$n(x) = n_i e^{(\psi(x)-\phi_F)/\phi_T} \quad (12)$$

where $n(x)$, n_i , $\psi(x)$, respectively, are the electron concentration at x position, the intrinsic concentration, potential at x position.

In photosensitive BJMOSFET, we can similarly obtain the Boltzmann distribution

$$n_{surface} = n_i e^{(\psi_s-\phi_F)/\phi_T} \quad (13)$$

where $n_{surface}$ is the electron concentration at the surface.

In depletion region (which the photosensitive BJMOSFET operating in), $n_{surface}$ is not larger than n_i . As a consequence, Q_C is mainly due to Q_B , and Q_L can be ignored based on ideal assumption.

Accordingly, using (2), (10) and (11), equation (4) can be simplified as follows:

$$V_{GK} \approx V_{FB} + \psi_S + \gamma\sqrt{\psi_S} \quad (14)$$

Then, the surface potential ψ_S can be written as

$$\psi_S = \left(-\frac{\gamma}{2} + \sqrt{\frac{\gamma^2}{4} + V_{GK} - V_{FB}}\right)^2 \quad (15)$$

Equation (15) demonstrates that the V_{AK} has no effort to the surface potential in the depletion region. In the other word, the V_{AK} only present a high electric field, but no contribution to the variation of d_B .

III. Photoelectric Characteristics

In the following calculation of photoelectric characteristics in photo-BJMOSFET, electric constants used here are: q =1.602×10^{-19}C, h =6.625×10^{-34}, ε_{OX} = 3.45 ×10^{-13}F/cm, ε_S = 1.04×10^{-12}F/cm. The workfunction of ITO is equal to 4.95eV and the workfunction of P-si doping of 10^{15}cm^{-3} is equal to 4.93eV, thus, the $V_{FB} = \frac{\phi_{ms}}{q} = \frac{W_m - W_s}{q}$ =0.02V(the parasitic charge of oxide is ignored). From (2) and (4), using these parameters given above, we can yield V_T = 0.026V and γ =0.53. From standard equation in substrate $P_0 = N_A = n_i e^{\phi_F/\phi_T}$, we can get ϕ_F =0.289V. Due to the photosensitive BJMOSFET operating in depletion region bur not inversion region, from the (13), we can obtain $\psi_S \leq 2\phi_f$. Furthermore, from (14), we can get V_{GK} ≤1.0V. Fig.3 presents carriers concentration in the film. It can be seen that the concentration of electron at interface is equal to 10^{15}cm^{-3} (this indicates inversion region).

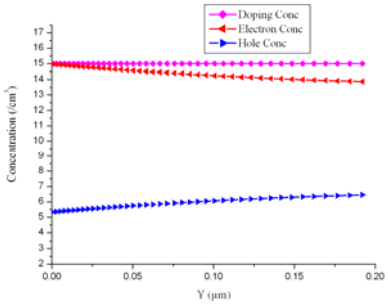

Fig. 3 Concentration of net doping, electron and hole in film at x=5μm when V_{GK} is equal to 1.0V and V_{AK} is equal to 0V.

3.1 Responsivity

We performed 2D Atlas simulations of photo-BJMOSFET with different V_{GK} . Typical results of photo-current to light intensity are depicted in Fig. 4. It is demonstrated that the photo-current increases rapidly at same light intensity from V_{GK}=0V to V_{GK}=1.0V. From (15), depletion region but not inversion region is formed in film under V_{GK}=0V to V_{GK}=1.0V to reduce recombination. However, in (14), influence of V_{AK} is ignored. Curves in Fig.4 corresponding to V_{GK} from 1.2V to 1.8V indicate that V_{AK} have effect to ψ_S and photo-current, but

the influence is very small (can be ignored). Strong inversion is formed in film due to increasing V_{GK} result in photo-current decreasing as curves corresponding to V_{GK}=2.1V and V_{GK}=2.4V presented in Fig.4. Therefore, the rang of V_{GK} is obtained from 0V to 1.0V in discussion here.

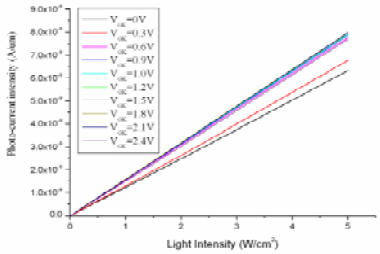

Fig. 4 Curves of photo-current to light intensity which ranges from 0W/cm^2 to 5w/cm^2 according to V_{GK}=0V, 0.3V, 0.6V, 0.9V, 1.0V, 1.2V, 1.5V, 1.8V, 2.1V and 2.4V, respectively. The wavelength of incident light, λ, is equal to *570nm*.

As can be seen in Fig.5, the responsivity increases along with increasing V_{GK}. At V_{GK}=0.1V, the responsivity is up to 20mA/W.

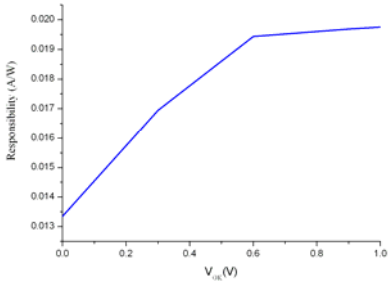

Fig. 5 Curve of responsivity vs. V_{GK} (which ranges from 0V to 1V) for L=8μm, L_{PN}=1μm, W=10μm, d_{si}=0.2μm, λ=570nm.

3.2 Sensitivity

It is demonstrated from equation (15), from V_{GK}=0V to 1.0V, the film under gate is in depletion region but not inversion region. In depletion region, the carrier concentration is lower than its equilibrium value and electrons and holes are then generated. At room temperature, the dark current of the photo-BJMOSFET is dominated by the thermal volume (Shockley–Read–Hall) and surface generation current. The contribution to the dark current of the other part of the device is indeed about four orders of magnitude lower[18]. Fig. 6 shows a very low value of dark currents to achieve a high ratio of more than 10^7 between photo to dark current. Thus, the minimum detectable power is lower than 10^{-7}W/cm^2.

3.3 Spectral response

To further investigate the photoelectric characteristics in detail, the spectral responses were simulated, as shown in Fig.7. As can be seen in Fig.7, full-widths at half-maximum (FWHM) at different V_{GK} are the same, which ranges from 290nm to 490nm. Just except the different photocurrent intensity due to different depletion situation.

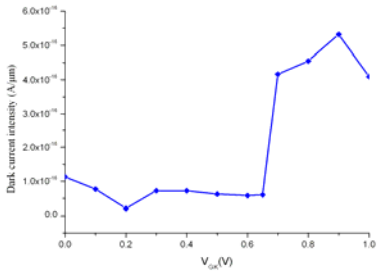

Fig. 6 Curve of dark current intensity vs. V_{GK} (which ranges from 0V to 1V) for L=8μm, L_{PN}=1μm, d_{si}=0.2μm, λ=570nm.

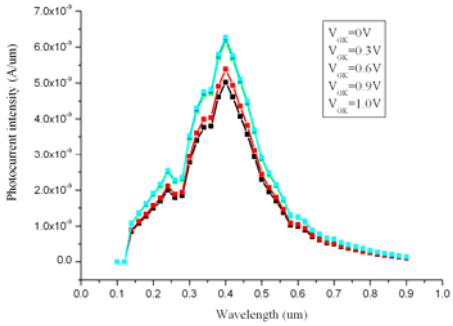

Fig. 7. Spectral responses corresponding to V_{GK}=0V, 0.3V, 0.6V, 0.9V and 1.0V, respectively.

The dark-current, photocurrent, and photo-to-dark-current ratios under 5W/cm^2 light intensity and their improvement ratios for photo-BJMOSFET are listed in Table I, which

TABLE I
DARK-CURRENT, PHOTOCURRENT, AND PHOTO-TO-DARK-CURRENT RATIOS UNDER 5W/CM^2 LIGHT INTENSITY AND THEIR IMPROVEMENT RATIOS FOR PHOTO-BJMOSFET WITH L=8μm, L_{PN}=1μm, D_{Si}=0.2μm.

V_{GK}	0V	0.3V	0.6V	0.9V	1.0V
Dark current(A) at W=10μm	1.13e-15	7.24e-16	5.85e-16	5.37e-15	4.81e-15
Improvement ratio in dark current	1	1.56	1.93	0.21	0.23
Photo current(A) at W=10μm	6.33e-8	6.78e-8	7.78e-8	7.87e-8	7.90e-8
Improvement ratio in photo current	1	1.07	1.23	1.24	1.25
Photo-to-dark-current ratio at W=10μm	5.6e7	9.36e7	1.33e8	1.45e7	1.64e7
Improvement ratio in photo-to-dark-current ratio	1	1.67	2.38	0.26	0.29

indicates that the greatest improvement in photo current is obtained at V_{GK}=1.0V. However, the greatest improvement in dark current appears at V_{GK}=0.6V and the greatest improvement in a photo-to-dark-current ratio is achieved also at V_{GK}=0.6V. Furthermore, the darkcurrent is increased a little when V_{GK}>0.6V, thus demonstrating that the weak inversion region is formed on the surface.

IV. Conclusion

ITO film which transmittancea is higher than 80% for λ from 500nm to 700nm is adopted as gate in photo-BJMOSFET fabricated on SOI film to reduce light absorption. Thin film is in depletion but not inversion region by gate voltage. Numerical simulations is performed by 2D Atlas corresponding to V_{GK}=0V, 0.3V, 0.6V, 0.9V and 1.0V with V_{AK} =1.0V for total area of $10\times10\mu m^2$. The greatest improvement to V_{GK}=0V (which is equivalent to lateral PIN but with lower reverse voltage) in dark current and in photo-to-dark-current ratio are up to 1.93 and 2.38, respectively, at V_{GK}=0.6V. The greatest improvement in photo-current (up to 1.25) is obtained at V_{GK}=1.0V. The FWHM ranges from 290nm to 490nm and the minimum detectable power is lower than $10^{-7}W/cm^2$. Furthermore, photo-BJMOSFET is propitious to integration for big input resistance. Consequently, photo-BJMOSFET fabricated on SOI film could be widely adopted in low dark current and responsive integrated photodetectors.

Acknowledgment

This work was supported by the Hunan Provincial Innovation Foundation for Postgraduate, National Natural Science Foundation of China (No. 90606009) and Hunan Provincial Natural Science Foundation of China (No.09JJ5041).

References

[1] K. Wang, Y. Vygranenko and A. Nathan, "Optically transparent ZnO-based n–i–p ultraviolet photodetectors" *Thin Solid Films*, vol515, pp. 6981-6985, June 2007.

[2] Csutak, S.M. Schaub, J.D. Wu, W.E. Shimer, R. Campbell, J.C., "CMOS-compatible high-speed planar silicon photodiodes fabricated onSOI substrates", *IEEE J Quantum Electron*. vol. 38, pp. 193-196, Feb 2002.

[3] S Nakaharai, T Tezuka, N Hirashita, E Toyoda, Y Moriyama, N Sugiyama, et al, "The generation of crystal defects in Ge-on-insulator (GOI) layers in the Ge-condensation process" *Semiconductor science and technology*. vol.22, pp. 26-28, Jan 2007.

[4] L Ke, XY Zhao, RS Kumar, SJ Chua," Low frequency optical noise from organic light emitting diode", *Solid-State Electronics*, vol. 52, pp. 7-10, Jan 2008.

[5] Afzalian A, Flandre D, " Speed performances of thin-film lateral SOI PIN photodiodes up to tens of GHz" *2006 IEEE International SOI Conference Proceedings*, pp.83-84 Oct. 2006

[6] S. G. Chamberlain, D. J. Roulston, S. P. Desai, "Spectral response limitation mechanisms of a shallow junction np photodiode" *IEEE Transactions on Electron Devices*, vol.13, pp. 167-172, Jan 1978.

[7] H.S. Wong, "Technology and device scaling considerations for CMOS imagers" *IEEE Trans.Electron Devices*, vol. 43, pp. 2131-2142, Dec 1996.

[8] N. H. Zhu, Y. Liu, S. J. Zhang, J. M. Wen, "Bonding-wire compensation effect on the packaging parasitics of optoelectronic devices" *Microwave and Optical Technology Letters*. vol.48, pp.76-79, Jan 2006.

[9] A. J. Blanksby, M. J. Loinaz, "Performance analysis of a color CMOS photogate image sensor" *IEEE Trans ,Electron Devices*, vol. 47, pp. 55-64, Jan 2000.

[10] Fábio Alencar Mendonça, Rubens Viana Ramos, "Optical receiver for instrumentation and communication" *Microwave and Optical Technology Letters*, vol. 45, pp. 415-419, May 2005.

[11] Z. Dilli, N. Goldsman, M. Peckerar, A. Akturk and G. Metze, "Design and testing of a self-powered 3D integrated SOI CMOS system" *Microelectronic Engineering*, vol.85, pp. 388-394, Feb 2008.

[12] Csutak SM, Dakshina-Murthy S, Campbell JC, "CMOS-compatible planar silicon waveguide-grating-couplerphotodetectors fabricated on silicon-on-insulator (SOI) substrates" *IEEE J Quantum Electron*, vol. 38, pp. 477-480, May 2002.

[13] M Ghioni, F Zappa, VP Kesan, J Warnock, "A VLSI-compatible high-speed silicon photodetector for optical data link applications" *IEEE Trans. Electron Devices*, vol. 43, pp. 1054–1060, June 1996.

[14] Afzalian A, Flandre D, "Physical modeling and design of thin-film SOI lateral PIN photodiodes" *IEEE Trans Electron Dev.* vol. 52, pp. 1116–1122, June 2005.

[15] Afzalian A, Flandre D, "Speed performances of thin-film lateral SOI PIN photodiodes up to tens of GHz" *IEEE Electron Lett*, vol. 42, pp. 1420–1421, Nov 2006.

[16] Afzalian A, Flandre D, "Characterization of quantum efficiency, effective lifetime and mobility in thin film ungated SOI lateral PIN photodiodes " *Solid-State Electronics*, vol.51, pp.337-342, Feb 2007.

[17] R Li, JD Schaub, SM Csutak, JC Campbell, "A high-speed monolithic silicon photoreceiver fabricated on SOI" *IEEE Photon Technol. Lett*, vol.12, pp.1046-1048, Aug 2000.

[18] A.Kranti and G. Alastair Armstrong, "Source/drain extension region engineering in nanoscale double gate SOI MOSFETs: Novel design methodology for low-voltage analog applications " *Microelectronic Engineering*, vol.84, pp. 2775-2784, Dec 2007

Hai-Qing Xie was born in Hunan, P.R.China, in 1982. He received the degree of Master of Science in Microelectronics and Solid-State Electronics in Hunan University in 2004. He is currently pursuing the Ph.D. degree at the same university, working on optical detectors.

His main research interests concern semiconductor optoelectronic material device and its application